

ite technical note techn

Effects of Ventilation and Panel Properties on Temperature Rise from Aircraft Fires

Thor I. Eklund

January 1984

DOT/FAA/CT-TN83/63

Document is on file at the Technical Center Library, Atlantic City Airport, N.J. 08405



U.S. Department of Transportation
Federal Aviation Administration

Technical Center
Atlantic City Airport, N.J. 08405

1. Report No. DOT/FAA/CT-TN83/63		2. Government Accession No.		3. Recipient's Catalog No.	
4. Title and Subtitle EFFECTS OF VENTILATION AND PANEL PROPERTIES ON TEMPERATURE RISE FROM AIRCRAFT FIRES				5. Report Date January 1984	
				6. Performing Organization Code ACT-350	
7. Author(s) Thor I. Eklund				8. Performing Organization Report No. DOT/FAA/CT-TN83/63	
9. Performing Organization Name and Address Federal Aviation Administration Technical Center Atlantic City Airport, New Jersey 08405				10. Work Unit No. (TRAIS)	
				11. Contract or Grant No. T1702C	
12. Sponsoring Agency Name and Address U.S. Department of Transportation Federal Aviation Administration Technical Center Atlantic City Airport, New Jersey 08405				13. Type of Report and Period Covered Technical Note May - November 1983	
				14. Sponsoring Agency Code	
15. Supplementary Notes					
16. Abstract A simple model is developed to describe the performance of interior aircraft honeycomb panels in a fire environment. A perfect stirrer analysis is applied to an aircraft cabin in-flight fire of constant size. Heat addition from the fire is offset by heat losses through the aircraft ventilation system and heat transfer through wall and ceiling panels. The ventilation rate is generalized into an effective ventilation rate that includes the panel heat transfer losses. The analysis demonstrates that conduction heat transfer and convection heat transfer can play comparable roles in lowering asymptotic values of enclosure temperature rise. The analysis leads to the definition of both a characteristic ventilation time and a characteristic burning time. The ratio of these times is a dimensionless variable that dominates asymptotic values of temperature. Pyrolysis of panels is further demonstrated as a potential heat sink. An experimental technique is proposed to determine the thermal inertia of a fuselage interior in a non-destructive fashion.					
17. Key Words Aircraft Fire Heat Transfer Ventilation Pyrolysis			18. Distribution Statement Document is on file at the Technical Center Library, Atlantic City Airport, New Jersey 08405		
19. Security Classif. (of this report) Unclassified		20. Security Classif. (of this page) Unclassified		21. No. of Pages 23	22. Price

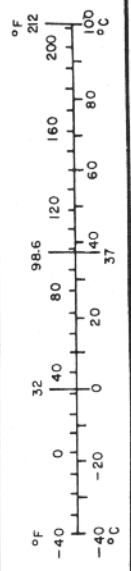
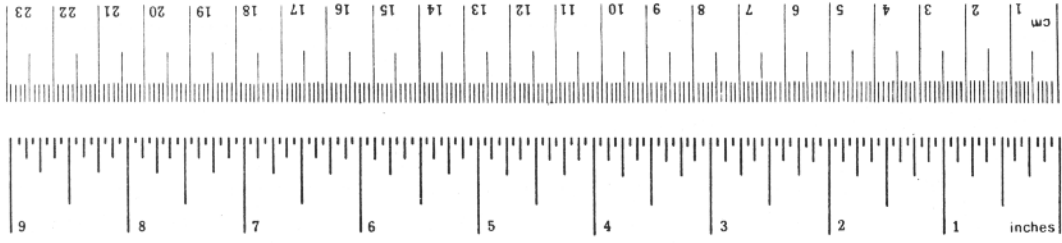
METRIC CONVERSION FACTORS

Approximate Conversions to Metric Measures

Symbol	When You Know	Multiply by	To Find	Symbol
LENGTH				
in	inches	*2.5	centimeters	cm
ft	feet	30	centimeters	cm
yd	yards	0.9	meters	m
mi	miles	1.6	kilometers	km
AREA				
in ²	square inches	6.5	square centimeters	cm ²
ft ²	square feet	0.09	square meters	m ²
yd ²	square yards	0.8	square meters	m ²
mi ²	square miles	2.6	square kilometers	km ²
	acres	0.4	hectares	ha
MASS (weight)				
oz	ounces	28	grams	g
lb	pounds	0.45	kilograms	kg
	short tons (2000 lb)	0.9	tonnes	t
VOLUME				
tsp	teaspoons	5	milliliters	ml
Tbsp	tablespoons	15	milliliters	ml
fl oz	fluid ounces	30	milliliters	ml
c	cups	0.24	liters	l
pt	pints	0.47	liters	l
qt	quarts	0.95	liters	l
gal	gallons	3.8	liters	l
ft ³	cubic feet	0.03	cubic meters	m ³
yd ³	cubic yards	0.76	cubic meters	m ³
TEMPERATURE (exact)				
°F	Fahrenheit temperature	5/9 (after subtracting 32)	Celsius temperature	°C

Approximate Conversions from Metric Measures

Symbol	When You Know	Multiply by	To Find	Symbol
LENGTH				
mm	millimeters	0.04	inches	in
cm	centimeters	0.4	inches	in
m	meters	3.3	feet	ft
m	meters	1.1	yards	yd
km	kilometers	0.6	miles	mi
AREA				
cm ²	square centimeters	0.16	square inches	in ²
m ²	square meters	1.2	square yards	yd ²
km ²	square kilometers	0.4	square miles	mi ²
ha	hectares (10,000 m ²)	2.5	acres	acres
MASS (weight)				
g	grams	0.035	ounces	oz
kg	kilograms	2.2	pounds	lb
t	tonnes (1000 kg)	1.1	short tons	short tons
VOLUME				
ml	milliliters	0.03	fluid ounces	fl oz
l	liters	2.1	pints	pt
l	liters	1.06	quarts	qt
l	liters	0.26	gallons	gal
m ³	cubic meters	35	cubic feet	ft ³
m ³	cubic meters	1.3	cubic yards	yd ³
TEMPERATURE (exact)				
°C	Celsius temperature	9/5 (then add 32)	Fahrenheit temperature	°F



* 1 in = 2.54 (exact). For other exact conversions and more detailed tables, see NBS Misc. Publ. 286, Units of Weights and Measures, Price \$2.25, SD Catalog No. C13.10-286.

TABLE OF CONTENTS

	Page
EXECUTIVE SUMMARY	v
INTRODUCTION	1
Purpose	1
Background	1
Objectives	2
ANALYSIS	2
The Case of Adiabatic Walls	2
The Case of Nonadiabatic Walls	2
Fractional Heat Loss to Walls	6
Pyrolysis of The Panels	14
Applications to Testing	16
DISCUSSION	17
CONCLUSIONS	18
REFERENCES	18

LIST OF ILLUSTRATIONS

Figure		Page
1	Control Volume	3
2	Hypothetical Enclosure	11
3	Characteristic Temperature Growth	13
4	Idealized Panel Construction	14

EXECUTIVE SUMMARY

Experimental and analytic work on aircraft fires have emphasized fire spread rates and energy release rates of burning aircraft materials. Both of these are needed to estimate heat production from an in-flight fire. Much less attention has been placed on heat loss mechanisms in the aircraft interior. The latter issue is important because the thermal growth observed in the fuselage cabin reflects the time history of difference between heat production and heat loss. Thus, a systems approach to improving the fireworthiness of an enclosure could involve maximizing heat losses as well as minimizing flammability.

A perfect stirrer analysis was used to evaluate the relative roles played by the following heat loss mechanisms: (a) the aircraft ventilation system, (b) the conductivities of interior panels, and (c) the energy sink effects caused by panel pyrolysis. The analysis generated three critical characteristic times. The characteristic burning time is inversely related to fire size, the characteristic ventilation time is inversely related to the ventilation rate, and the effective time for an air change includes combined ventilation heat losses and wall heat transfer. The overall analysis further suggests an experimental non-destructive technique for determining the thermal inertia of a fuselage interior.

The conclusions resulting from the analysis are that conductive heat losses and ventilation can play comparable roles in cooling the fuselage, that data taken at outflow values can provide valuable overall diagnostic material, and that conductivity values of lining materials are necessary ingredients to overall analysis of in-flight fire development.

INTRODUCTION

PURPOSE.

The purpose of this analysis is the development of a simple model that describes the performance of interior aircraft panels in a fire environment. The analysis consists of an examination of the interactions of ventilation and interior material properties in the development of thermal hazards from an idealized in-flight fire.

BACKGROUND.

In-flight fires represent a severe threat because of the time that may be required for landing the aircraft after the fire has been detected. In the process of descending, the rate at which the cabin environment deteriorates is affected not only by growth of the fire but also by ventilation effects and the interaction of interior materials with hot gases from the fire plume. In work on room fires (references 1 and 2), it has been estimated that something like 60 percent of the heat released by the fire ends up in heat transferred to the enclosure walls. The balance is carried away by gas phase motions. In that particular scenario, the room walls are generally something like gypsum. Besides the computational difficulties of computing the unsteady heat transfer to such walls, there are unknowns relating to the effects of moisture content in the wall. Additionally, in this room scenario, the ventilation rate is controlled by the fire itself. The fire results in a pressure differential between the smokey upper layer and the atmosphere outside any open door or window. It is this pressure differential that controls the movement of fresh air into the enclosure and the residence time associated with gas movement. With a given size fire, the wall heat transfer effects and the movement of gas into the enclosure play dominant roles in the development of the thermal hazard.

Focusing on these two effects, wall heat transfer and ventilation, we see clear differences in the case of large passenger aircraft. The ventilation is prescribed by the aircraft environmental control system rather than fire-induced natural convection. The ventilation rate can be as large as one air change every three minutes in the passenger section. Since the air enters at the ceiling and leaves at the floor level along the sidewalls, the possibility arises that the cabin can be treated as a perfect stirrer in a first order analysis of fire behavior. In contrast to a typical building enclosure, the aircraft walls and ceiling are often of a honeycomb-type construction with the following being typical of the state-of-the-art. A nomex honeycomb core is covered on each side with layers of resin impregnated fabric. On the cabin interior side of the panel, there are layers of polyvinyl fluoride covering the decorative ink. The walls potentially could thermally interact with the enclosed hot gases through the heat capacity of the wall materials, conduction of heat into and through the materials, and by pyrolysis of the materials.

Thus, the aircraft fire scenario will consist of two dominant aspects. First, the stirrer concept will cause mixing of the hot products of combustion with the cabin air, with some heat going to raise the air temperature and some heat exiting with the forced ventilation airflow. Second, the materials lining the walls will be analyzed for heat transfer losses up to the point of pyrolysis. At the time of pyrolysis, the materials will be treated as thin layers of materials which absorb heat only as they change phase or pyrolyze. In effect, a cabin fire will gradually

cause a temperature rise which is slowed by dilution with ventilation air and by heat transfer losses. When the cabin air temperature reaches a phase transition or polymer decomposition temperature, the temperature rise of the cabin air stops until enough heat is transferred to the wall layer for transition. The temperature of the gas continues to rise until another layer transition temperature is reached. Thus, under this analytical approach, the ablative effects of wall lamina can be demonstrated. To keep the analysis as simple as possible, the many other materials in the cabin (seats, carpet, seat back trays, etc.) will be ignored so that panel behavior can be more clearly predicted.

This treating of the wall layers as heat sinks during transitions is founded in applications of the Spalding B number. The Spalding B number is basically a ratio of a substance's heat of combustion to the heat absorbed by the substance in being raised to a phase change temperature and changing phase. In many applications, the energy involved in the phase change is much greater than that involved in heating the material to the phase change temperature. Then, the Spalding B number is proportional to the heat of combustion divided by the heat of vaporization. Because of the high vertical velocities in the vicinity of a fire plume, the stirrer approximation cannot be expected to be realistic near the fire plume. Rather, the analysis may serve to describe gross processes elsewhere in the enclosure.

OBJECTIVE.

The objective of the analysis is to develop the relationship of ventilation rate, fire size, and material properties in such a manner that (1) full-scale and small-scale fire tests can be designed as to optimal variables for data collection and (2) panel design characteristics that affect fire performance are identified. If the perfect stirrer approach is valid for fires under conditions of forced ventilation, then the most effective location to acquire data to diagnose the cabin environment would be at the cabin outflow locations.

ANALYSIS

THE CASE OF ADIABATIC WALLS.

The analysis begins with the case of a perfectly stirred ventilated compartment with adiabatic walls. This is a case where no heat is lost to the walls. Although wall heat transfer is an integral part of the complete treatment, the adiabatic case allows clear isolation of some significant parameters and additionally serves as a primary building block of the final solution.

Figure 1 shows the control volume for the ventilated compartment. A heat balance simply says that the enthalpy added by incoming ventilation plus the enthalpy added by the fire equals the accumulation of enthalpy plus the enthalpy that leaves the enclosure through the ventilation system. Symbolically, this can be written as follows:

$$\dot{m}_B \Delta H_c + \frac{a}{A_0} M C_p (T_0 - T_R) \quad (1)$$

$$= \frac{m}{A_0} M C_p (T - T_R) + \frac{d}{dt} \left[\frac{a}{A_0} M C_p (T - T_0) \right]$$

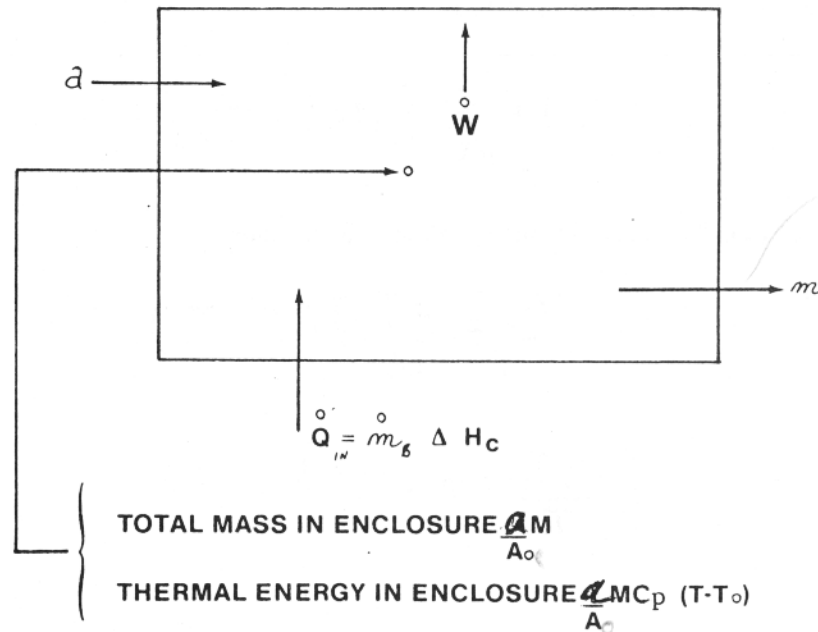


FIGURE 1. CONTROL VOLUME

where \dot{m}_B is the material burning rate, ΔH_c is the heat of combustion, M is the average molecular weight of the gas, A_0 is Avagadro's number, a is the number of molecules entering the enclosure, C_p is the specific heat, T_0 is the temperature of gas entering the enclosure, T_R is a reference temperature, m is the number of molecules leaving the enclosure, T is the temperature within the enclosure, and a is the number of molecules within the enclosure. If the reference temperature is chosen equal to T_0 , equation (1) simplifies to;

$$\dot{m}_B \Delta H_c - \frac{m}{A_0} M C_p (T - T_0) = \frac{d}{dt} \left[\frac{a}{A_0} M C_p (T - T_0) \right] \quad (2)$$

Equation 2 shows the result of the perfect stirrer assumption where the compartment temperature T is also the temperature of the outflow gas at any instant of time. The continuity equation states;

$$a - m = \frac{d}{dt} a \quad (3)$$

Furthermore, assuming constant pressure in the enclosure, the perfect gas law states;

$$aT = a_0 T_0 \quad (4)$$

Combining (3) and (4) leads to

$$m = a + \frac{a_0 T_0}{T^2} \frac{dT}{dt} \quad (5)$$

and this shows that as the enclosure temperature rises, the number of molecules flowing out exceeds the number flowing in as a result of thermal expansion. Equation 2 can be rearranged as follows:

$$\frac{A_0 \dot{m}_B \Delta H_c}{M C_p} = m (T - T_0) + \frac{d}{dt} [a(T - T_0)] \quad (6)$$

Equations 4 and 5 can be used with equation 6 to make

$$\begin{aligned} \frac{A_0 \dot{m}_B \Delta H_c}{M C_p} &= \left(a + \frac{a_0 T_0}{T^2} \frac{dT}{dt} \right) (T - T_0) \\ &+ \frac{d}{dt} \left[\frac{a_0 T_0}{T} (T - T_0) \right] \end{aligned} \quad (7)$$

Equation 7 reduces to:

$$\frac{A_0 \dot{m}_B \Delta H_c}{M C_p} + 2 T_0 = T \left(a + \frac{a_0 T_0}{T^2} \frac{dT}{dt} \right) \quad (8)$$

Equation 8 can be rearranged to show:

$$\frac{dT}{dt} = \frac{T \left(\frac{A_0 \dot{m}_B \Delta H_c}{M C_p} + 2 T_0 \right)}{a_0 T_0} - \frac{T^2 a}{a_0 T_0} \quad (9)$$

Further rearrangement leads to:

$$\frac{dT}{\frac{T \left(\frac{A_0 \dot{m}_B \Delta H_c}{M C_p} + 2 T_0 \right)}{a_0 T_0} - \frac{T^2 a}{a_0 T_0}} = dt \quad (10)$$

Equation 10 can be integrated to get:

$$- \left[\frac{\left(\frac{A_0 \dot{m}_B \Delta H_c}{M C_p} + a T_0 \right)}{a_0 T_0} \right] \ln \left[\frac{\frac{A_0 \dot{m}_B \Delta H_c}{M C_p} + a T_0}{a_0 T_0} - \frac{a T}{a_0 T_0} \right]$$

$$= \tau + C \quad (11)$$

Taking the exponential of both sides of equation 11, the following arises:

$$\frac{\frac{A_0 \dot{m}_B \Delta H_c}{M C_p} + a T_0}{a_0 T_0} - \frac{a T}{a_0 T_0}$$

$$= T B \exp \left[- \frac{t \left(\frac{A_0 \dot{m}_B \Delta H_c}{M C_p} + a T_0 \right)}{a_0 T_0} \right] \quad (12)$$

Since $T = T_0$ at $t = 0$, the integration constant B can be defined:

$$B = \frac{A_0 \dot{m}_B \Delta H_c}{M C_p a_0 T_0^2} \quad (13)$$

Since $M a_0/A_0$ is nothing other than the initial weight of air in the enclosure, $\rho_0 V$, and since a_0/a is the prescribed time for an air change, τ , equation (12) can be written in more conventional terms as:

$$\frac{\dot{m}_B \Delta H_c}{\rho_0 V C_p T_0} + \frac{1}{\tau} - \frac{1}{\tau} \frac{T}{T_0} \quad (14)$$

$$= \frac{T}{T_0^2} \frac{\dot{m}_B \Delta H_c}{C_p \rho_0 V} \exp \left[- t \left(\frac{\dot{m}_B \Delta H_c}{\rho_0 V C_p T_0} + \frac{1}{\tau} \right) \right]$$

Calling τ a characteristic ventilation time suggests defining a characteristic burning time, τ_B , as follows:

$$\tau_B = \frac{\rho_0 V C_p T_0}{\dot{m}_B \Delta H_c} \quad (15)$$

In this way equation 14 simplifies further to:

$$\frac{1}{\tau_B} + \frac{1}{\tau} \left(1 - \frac{T}{T_0}\right) = \frac{T}{T_0} \cdot \frac{1}{\tau_B} \exp \left[-t \left(\frac{1}{\tau_0} + \frac{1}{\tau} \right) \right] \quad (16)$$

This can be further manipulated to show the temperature more explicitly:

$$\frac{T}{T_0} = \frac{\frac{1}{\tau_B} + \frac{1}{\tau}}{\frac{1}{\tau} + \frac{1}{\tau_B} \exp \left[-t \left(\frac{1}{\tau_0} + \frac{1}{\tau} \right) \right]} \quad (17)$$

Equation 17 is the equation of heat rise for a fire of constant size in a forced ventilated enclosure with adiabatic walls. For very large times, t is much greater than $(1/\tau_B + 1/\tau)$, and the asymptotic expression for T becomes

$$T = T_0 \left(1 + \frac{\tau}{\tau_B} \right) \quad (18)$$

Thus, the final temperature is small when the time for an air change is small or when the characteristic burning time is large.

THE CASE OF NONADIABATIC WALLS.

In the more realistic case which allows the enclosure gas to transfer heat to the walls, equation 2 takes the form:

$$\dot{m}_B \Delta H_c - \frac{\dot{m}}{A_0} M C_p (T - T_0) - \dot{W}$$

$$= \frac{d}{dt} \left[\frac{a}{A_0} M C_p (T - T_0) \right] \quad (19)$$

where \dot{W} represents the heat loss to the walls. Expanding terms and substituting in the same fashion used to develop equation 7 results in equation 19 becoming:

$$\frac{A_0 \dot{m}_B \Delta H_c}{M C_p} + a T_0$$

$$= \frac{\dot{W} A_0}{M C_p} + T \left(\dot{a} + \frac{a \cdot T_0}{T^2} \frac{dT}{dt} \right) \quad (20)$$

Solutions to equation 20 depend on the form taken by \dot{W} .

Identification of \dot{W} in principle involves knowledge of gas phase heat transfer coefficients, specific heat of the wall material, and thermal conductivity of the wall material. This kind of information is very scarce. Nevertheless, correlation techniques that have been successfully used for room fire analysis can be applied to the aircraft problem. Reference 3 gives the following two approximations for wall conductance, h_k :

$$h_k = \sqrt{\frac{k \rho c}{t}} \quad , \quad t \leq t_p \quad (21)$$

$\sqrt{\frac{k \rho c}{t_p}} = \frac{k}{\delta}$

$$h_k = \frac{k}{\delta} \quad , \quad t \geq t_p \quad (22)$$

$\frac{k \rho c}{t_p} = \frac{k^2}{\delta^2}$
 $\therefore t_p = \frac{\rho c}{k}$

where k is the thermal conductivity of the wall, ρ is the wall density, c is the wall heat capacity, δ is the wall thickness, and t_p is a solid thermal penetration time defined as

$$t_p = \left(\frac{\rho c}{k} \right) \left(\frac{\delta}{2} \right)^2 \quad (23)$$

Equation 21 approximates heat flow to the wall during the time interval when the wall itself is absorbing significant heat. Equation 22 approximates the case where heat loss to the wall is exclusively from heat conduction through it.

To use these equations, both the thermal conductivity and the grouping $k\rho c$ must be known. Then the wall heat loss term in equation 20 can be written as

$$\dot{W} = h_k S (T - T_0) \quad (24)$$

where S is in the total wall surface, and h_k takes the appropriate form from equation 21 and 22. The determination which of these equations to use depends on the thermal penetration time, t_p . Reference 4 contains an empirical approach for determining $k\rho c$ from flame spread experiments. In the analysis from reference 4, two of the equations are needed to draw $k\rho c$ from the flame spread data. They are the following:

$$\dot{q}_{MIN} = h (T_{ig} - T_i) \quad (25)$$

and

$$a = \frac{h^2}{k\rho c} \quad (26)$$

where \dot{q}_{min} is the minimum external heat flux to the material for ignition over a long time of preheating, h is the convective heat transfer coefficient from the material, T_{ig} is the material surface temperature at ignition, T_i is the initial temperature or the ambient temperature, and a is an empirical parameter leading to best fit of the data.

One of the materials tested was a reasonably representative aircraft panel with the following intrinsic and measured properties:

$$S = 2.54 \text{ cm}$$

$$a = 0.05 \text{ sec}$$

$$\rho = 126 \text{ kg/m}^3$$

$$T_{ig} = 536^\circ\text{C}$$

$$\dot{q}_{MIN} = 2.7 \text{ w/cm}^2$$

From these values, equations 25 and 26 show that $h = 0.0528 \text{ kw/m } ^\circ\text{C}$ and finally $k\rho c = 0.055 (\text{kw/m}^2\text{ } ^\circ\text{C})^2\text{sec}$. To develop the thermal penetration time, it is necessary to define the conductivity, k . Most solid materials have a heat capacity, c , very close to $1.0 \text{ kJ/kg } ^\circ\text{K}$, and references 3 and 5 bracket this with values of $1.26 \text{ kJ/kg } ^\circ\text{K}$ for a representation polymer composite and $0.8 \text{ kJ/kg } ^\circ\text{K}$ for glass fiber insulation, respectively. Thus, use of the unitary value is a reasonable approximation. Using these values, the thermal conductivity of the panel comes out to be $0.437 \text{ w/m } ^\circ\text{C}$.

Thus, the thermal penetration time for the panel evaluated in reference 4 would be 46.5 seconds. Panels of practical interest are more likely to be in the range of $1/4$ inch to $1/2$ inch, and more typical thermal penetration times would be between $1/16$ and $1/4$ of the calculated 46.5 seconds because of the fact that t_p goes like δ^2 . Because the overall time frames of the heating problem under consideration here are of the order of minutes, equation 22 describes the heat transfer to the walls for almost all time up to pyrolysis. For this problem, this indicates that the panels have virtually no heat capacity but rather take heat from the cabin by conduction through the panel to the backface. Thus, equation 24 can be written as

$$\dot{W} = \frac{k}{s} \delta (T - T_0) \quad (27)$$

In this equation we are assuming that the area behind the panel stays at T_0 . Inserting equation 27 into equation 20 leads to the following equation:

$$\begin{aligned} \frac{A_0 \dot{m}_g \Delta H_c}{M C_p} + a T_0 - \frac{k}{s} \frac{\delta A_0}{M C_p} (T - T_0) \\ = T \left(a + \frac{a_0 T_0}{T^2} \frac{dT}{dt} \right) \end{aligned} \quad (28)$$

This can be rearranged to

$$\begin{aligned} \frac{A_0 \dot{m}_g \Delta H_c}{M C_p} + a' T_0 \\ = T \left(a' + \frac{a_0 T_0}{T^2} \frac{dT}{dt} \right) \end{aligned} \quad (29)$$

where

$$a' = a + \frac{k}{s} \frac{\delta A_0}{M C_p} \quad (30)$$

Equation 29 is identical to equation 8 and the same solution will be obtained. That is

$$\frac{T}{T_0} = \frac{\frac{1}{\tau_B} + \frac{1}{\tau'}}{\frac{1}{\tau'} + \frac{1}{\tau_B} \exp \left[-t \left(\frac{1}{\tau_B} + \frac{1}{\tau'} \right) \right]} \quad (31)$$

Where τ' is a_0/a' . Thus, the ventilation time constant has been generalized to include within itself the heat conducted out of the cabin through the panels.

Rewriting this non-adiabatic time constant τ' as

$$\tau' = \frac{1}{\frac{1}{\tau} + \frac{k \delta A_0}{S M a_0 C_p}} \quad (32)$$

the relative roles of ventilation and heat conduction in cooling the cabin can be shown in specific cases. For a 1/2 inch panel in a hypothetical configuration (figure 2) of two walls and a ceiling bounding an enclosure 16 feet wide, 8 feet high, and 100 feet long, $k \delta / S$ would be 13.5×10^2 watts/ $^{\circ}\text{C}$. Assuming an air change every three minutes for τ and a value of 203 Btu/ $^{\circ}\text{C}$ for the heat capacity of the air in the fuselage (that is, the value of $\frac{M a_0 C_p}{A_0}$), then

$$\tau' = \frac{1 \text{ min}}{0.33 + 0.32} \quad (33)$$

Thus, in this example, the walls and the ventilation perform roughly equal shares of the cooling. Even though the ventilation rate is once every 3 minutes, the effective rate is every 1.5 minutes. It is clear from equation 32 that the thinner that a panel is, the better will it remove heat and cool the enclosure. Thus, within the constraints of the assumptions made here, the solution for the case of the adiabatic wall apply to the non-adiabatic case as well so long as the time for an air change, τ , is replaced by an effective time, τ' .

The early form of equation 31 is of some interest in determining the rate of rise of temperature in an enclosure. For very small times, the exponential term can be approximated as

$$\exp \left[-t \left(\frac{1}{\tau_B} + \frac{1}{\tau'} \right) \right] \approx 1 - t \left(\frac{1}{\tau_B} + \frac{1}{\tau'} \right) \quad (34)$$

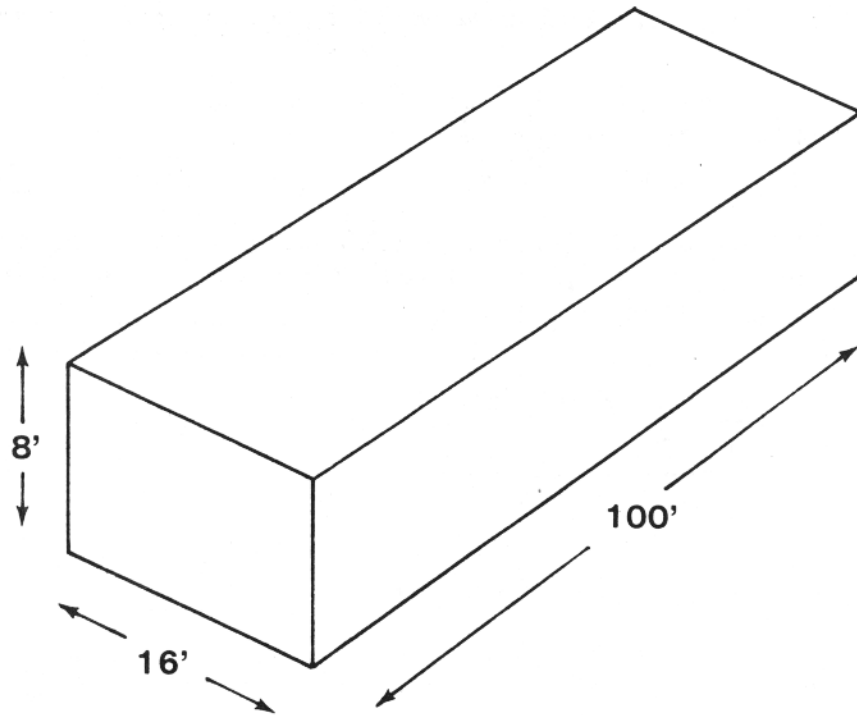


FIGURE 2. HYPOTHETICAL ENCLOSURE

Substituting equation 34 into equation 31 leads to the following relationship

$$\frac{T}{T_0} \approx \frac{\tau_B}{\tau_B - t} \quad (35)$$

Thus, the initial rate of temperature rise depends only on the characteristic burning time, τ_B .

FRACTIONAL HEAT LOSS TO WALLS.

The primary variables arising from this analysis are the characteristic times, τ_B , τ , and τ' . These times contain within themselves the burning rate, the ventilation rate, and the wall heat transfer respectively. In terms of design for fireworthiness, an option might be to transmit minimal or maximal heat through the panels. For long times, equation 31 shows

$$\frac{T}{T_0} = 1 + \frac{\tau'}{\tau_B} \quad (36)$$

From a practical viewpoint, this long time would be nearly reached when

$$t = 3 \left(\frac{1}{\tau_B} + \frac{1}{\tau'} \right)^{-1} \quad (37)$$

For instance, if τ' were 1.5 minutes and τ_B were 3 minutes, then at $t = 3$ minutes T/T_0 would be 95 percent of the asymptotic value. The ratio of the wall heat loss to the heat generated is

$$\frac{\dot{W}}{\dot{m}_B \Delta H_c} = \frac{\frac{k}{s} L (T - T_0)}{\dot{m}_B \Delta H_c} \quad (38)$$

Using the long time expansion, it follows that

$$T - T_0 = T_0 \left(\frac{\tau'}{\tau_B} \right) \quad (39)$$

Thus, defining τ_B explicitly shows

$$\frac{\dot{W}}{\dot{m}_B \Delta H_c} = \frac{k}{s} \frac{L}{\rho_0 V C_p} \tau' \quad (40)$$

What is significant here is that the long time fraction of heat transferred through the walls is independent of fire size and dependent only on the effective ventilation rate and the thermal properties of the gas in the enclosure and the properties of the panel. Using the values from the earlier example where k/s was 13.5×10^2 watts per degree and τ' was 1.5 minutes, the long time fractional heat transfer to the wall would be $0.3 \tau'$ per minute or 0.48. Thus, half the heat would be lost to the walls in this case.

Physically, what is going on in the overall situation is the following. At time zero when the fire starts, the overall enclosure is relatively cool inside so the differential temperature across the wall is small. Thus the leakage of energy by ventilation and conduction is small and enclosure temperature growth is fast. As the gas gets hotter, the temperature differentials get greater and larger fractions of produced heat are lost both by conduction and ventilation. It is these effects that slow the enclosure temperature growth and cause the characteristic shape shown in figure 3. Interestingly enough, this type shape was experimentally found for in-flight large scale tests described in reference 6. The long time temperature for a given fire size is clearly affected by the ventilation rates and the heat losses through the walls. If a fire can be controlled such that it remains at a modest size, the effective ventilation can potentially maintain the overall enclosure temperature to low enough values such that further material involvement is prevented.

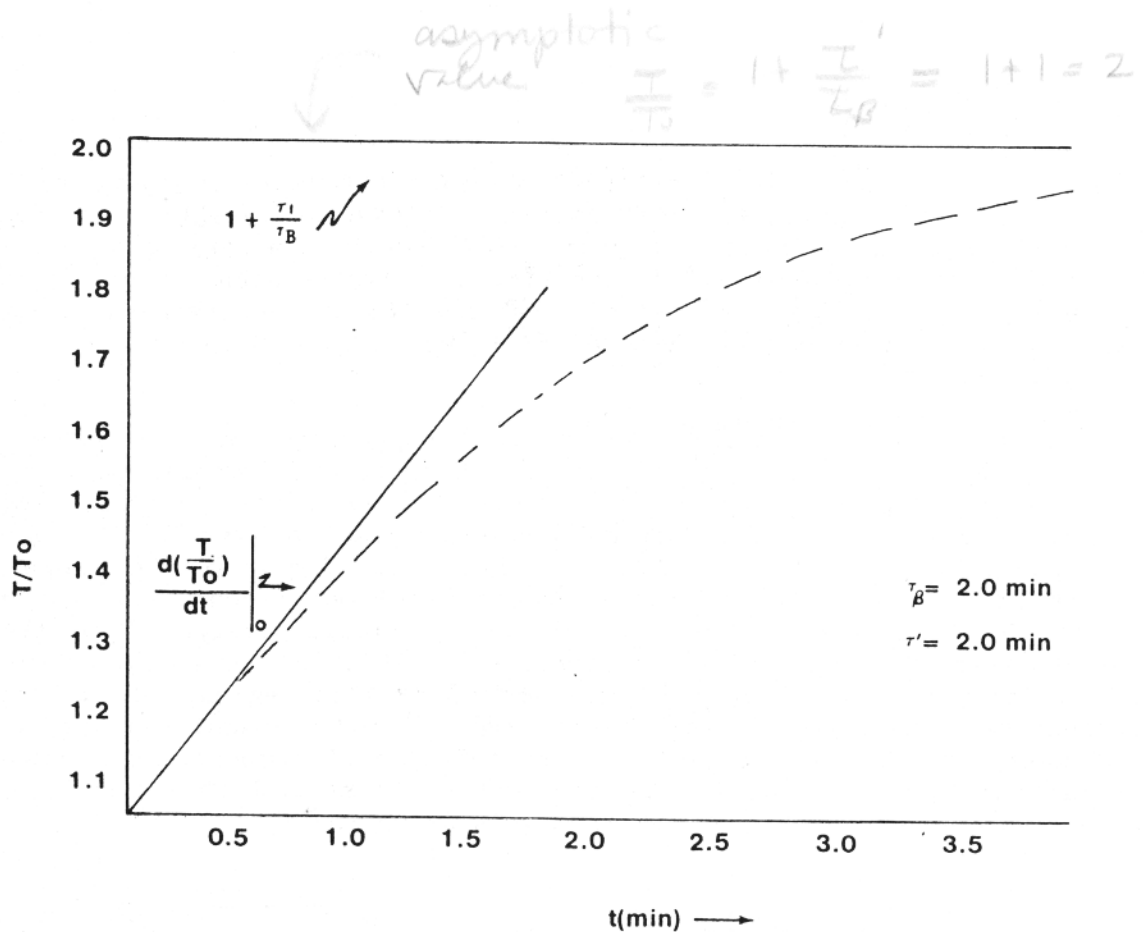


FIGURE 3. CHARACTERISTIC TEMPERATURE GROWTH

The long time fraction of heat transferred through the walls can be defined exclusively in terms of characteristic times if the definition equation 30 and 32 are used. The relationship is then

$$\frac{\dot{W}}{m \dot{v}_0 \Delta H_c} = 1 - \frac{T'}{T} \quad (41)$$

In the case of adiabatic walls, T' is identical to T and the long time fraction is zero. As the ratio of heat loss to the wall over heat loss to ventilation gets larger, T' gets smaller and the long time fraction of heat transferred through the walls gets larger. Heat fraction lost to the walls can be increased either by lowering T' through better conducting materials or by raising T through reduction of ventilation.

The empirical value of $k \rho c$ from reference 4 was used to predict heat transfer properties of panels of different thicknesses. More accuracy would accrue to these analyses if actual measurements of $k \rho c$ were available for 1/4 inch panels and 1/2 inch panels.

PHROLYSIS OF THE PANELS

The analysis up to this point includes steady state heat generation and unsteady heat losses through ventilation and conduction through the walls. As long as the panels remain chemically inert, the heat losses will be associated with convection and conduction of heat. However, if the fire is large enough so that the long time temperature, $T_o (1 + \gamma/\gamma_g)$, is greater than the temperature needed to degrade or pyrolyze the panel components, then an additional energy sink will be involved in the enclosure energy balance.

Figure 4 shows a model honeycomb panel. For simplicity, four regions are identified. Region 1 is the decorative protective surface (typically polyvinyl fluoride). Region 2 is a second lamina (typically epoxy or phenolic impregnated fiberglass). Region 3 is the honeycomb core (typically Nomex™) and region 4 is generally a lamina similar to that in region 2. For a simple approach, the assumption is that each region has a specific polymer decomposition temperature which will be designated as P_1 , P_2 , P_3 , and P_4 respectively. When the region reaches its respective decomposition temperature, it undergoes an endothermic pyrolysis that continues until only a char remains of that region. In reality, such transitions may occur over a temperature range of modest magnitude, but the artifice of making the energy release a delta function of temperature is convenient. It is further assumed that $P_1 < P_2 < P_3$ and it is stated that the approach is probably reasonable only through the pyrolysis of region 2.

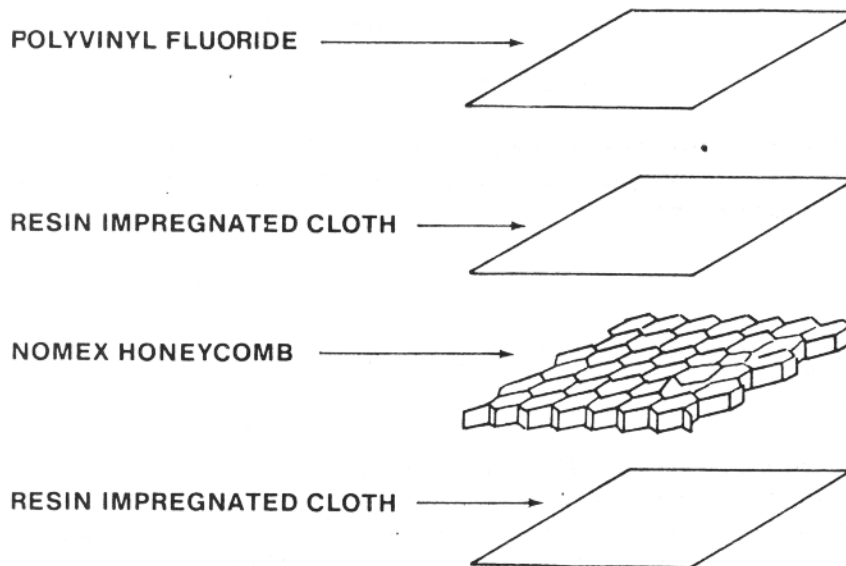


FIGURE 4. IDEALIZED PANEL CONSTRUCTION

Physically, once the polymer decomposition temperatures are defined, the pyrolysis model consists of allowing the enclosure temperature to rise via equation 31 until the enclosure temperature reaches P_1 . The enclosure temperature remains at P_1 until the first region is reduced to char. The enclosure continues to rise in temperature until P_2 is achieved. The enclosure then remains at temperature P_2 until region 2 is reduced to char.

*how do you know when
region is reduced completely
to char?*

During these transitions equation 24 is modified to include the endothermic reaction in the following manner:

$$\frac{A_o \dot{m}_B \Delta H_c}{M C_p} + a' (T_o - P_i) = \frac{Q_p A_o}{M C_p} \quad (42)$$

when the enclosure gas remains at the temperature of the particular transition, P_i , and where Q_p is the rate of energy transferred to the pyrolysis endotherm.

Given the total enclosure surface of panel as S and a polymer decomposition energy of L_i on a unit mass basis, the total decomposition energy involved at P_i would be $\rho_i d_i S L_i$ where ρ_i is the lamina density and d_i is its thickness. The time for this transition to take place is Δt_i and the total event can be described as follows:

$$Q_p \Delta t_i = \rho_i d_i S L_i \quad (43)$$

Using equation 43 in 42, the time for the pyrolysis of the i th lamina is

$$\Delta t_i = \frac{\rho_i d_i S L_i}{\dot{m}_B \Delta H_c - \frac{M C_p a'}{A_o} (P_i - T_o)} \quad (44)$$

Equation 44 states that the time for the enclosure to remain at temperature P_i is simply the heat required to pyrolyze the i th lamina divided by the net energy input from the fire source. The net energy is the heat of combustion minus the heat lost through ventilation and wall conduction. The equation shows that the enclosure potentially can be held at a temperature during pyrolysis of a lamina and, thereby, further temperature rise can be deferred. In terms of human survivability, advantages would accrue if the polymer decomposition temperature, P_i , were somewhat lower than 400°F . Higher temperatures would mean that the enclosure heat would both incapacitate occupants and cause autoignition of cellulosic contents. Additionally, the mass production of the pyrolysis products would have to be evaluated against ventilation rate to ensure that the pyrolysis products were not causing an ignitable fuel air mixture in the gas phase.

This point is brought out by consideration of a panel made of tedlar, phenolic/fiberglass, and Nomex honeycomb. The PVF and phenolics have polymer decomposition temperatures of 360°C (680°F) to 400°C (752°F). Thus, before these materials

would pyrolyze, the enclosure would be so hot that human survivability would be impossible. On the other hand, epoxy might have a polymer decomposition temperature in the neighborhood of 180° C (356° F). In fire tests of a PVC, epoxy/fiberglass, Nomex honeycomb panel, tedlar generally peels away and falls to the floor and this is probably due to the fact that the epoxy P_i is lower than that of tedlar. For such a panel system the model would allow only the epoxy/fiberglass lamina to decompose.

The type time intervals available from this pyrolysis event can be demonstrated in an example. The hypothetical enclosure of figure 2 has a total surface area of 3,200 square feet. Assuming a wall panel weight of 56 ounces per square yard, the total panel weight would be 1,200 pounds. The epoxy lamina below the tedlar might be something like twenty percent of the overall weight or 240 pounds. A typical heat of degradation of a polymer might be 300 calories per gram. According to the model proposed here, the enclosure would heat according to equation 31 until the air inside reached a temperature of 356° F. The enclosure would remain at 356° F for the time interval shown by equation 44.

To further specify the sample exercise, the following quantities are used:

$$\dot{m}_B \Delta H_c \quad : \quad 50,000 \text{ Btu/min}$$

$$M C_p a' (P_i - T_o) / A_o \quad : \quad 26,781 \text{ Btu/min}$$

$$P_i d_i \& L_i \quad : \quad 129,705 \text{ Btu}$$

Using these quantities, Δt_i comes out as 5.6 minutes. The numbers used roughly correspond to a strong seat fire, an air change every three minutes, and wall heat transfer characteristics developed previously for a 1/2-inch thick panel.

The phenomenon of cooling the enclosure in this fashion could be called ablation in a general sense. However, true ablative cooling refers to a situation where the back side of the panel in this exercise bounded the enclosure of interest.

APPLICATIONS TO TESTING.

Besides identifying the importance of definition of ventilation rate and lining materials in fire testing, the technique offers a way of defining the effective thermal inertia of a fuselage. The thermal inertia is related to τ' up to the point of pyrolysis or polymer degradation. As shown in equation 32 τ' is related only to the ventilation rate and material thermal properties. On the other hand, τ_B according to equation 15 is related to the enthalpy of the air in the enclosure divided by the fire's heat release rate. Equation 36 shows that the long time temperature is related to τ' divided by τ_B .

These equations can be used to determine the thermal response of an enclosure in a non-destructive fashion. A small heater of constant convective heat output

could be placed in an enclosure. If the heat output were adjustable at known outputs and set to give a long time heat buildup of approximately 100° F, then τ_B would be identified.

At a specified ventilation rate, the temperature time history could be measured, and equation 36 would yield an empirical value of τ' for the entire enclosure. This same τ' would apply for cases of larger fires that would destroy the enclosure.

In this manner, changes in ventilation ducting and materials could be accomplished experimentally to develop configurations with the smallest empirical τ' .

DISCUSSION

The use of a perfect stirrer type approach to analyze aircraft cabin fire scenarios is not a new development. Similar approaches by the aircraft manufacturers are documented in references 6 and 7. Additionally, the developments in reference 8 use a stirrer type approach to characterize exponential fire growth for a number of burning materials. In all these references, some success in correlation between model results and experimental results is demonstrated. Nevertheless, comparison of the results with further analytic and experimental work is difficult. References 6 and 7 involve actual fuselages or fuselage simulators. Nonetheless, either the origins or definitions of the analytical expressions are not readily ascertainable or the experimental test bed is not fully defined as to wall linings, volume, or air change rate. At this point, an expression like equation 31 does produce the general shape of the experimental data found in reference 6. Additionally, some credibility is given the approach of using equation 44 in reference 9 where the ceiling temperature curve remains stable at the ceiling material's approximate polymer decomposition temperature until burn-through occurs.

Evaluation of the literature and typical full-scale test procedures really indicates that use of the approaches developed here require clear definition of all wall linings as well as documentation of fire burning rate, fuselage volume, and ventilation rate. What is clear from this analysis is that panel heat sink behavior and fuselage ventilation counteract the thermal growth in the enclosure caused by a fire. As such, ventilation and wall heat transfer effects must be identified if survivability times are to be derived when the fire source is known.

The perfect stirrer approach is global in nature and will break down in the vicinity of a strong fire plume. The stirrer approach really generates a gross average condition describing the enclosure fire history.

The development at this point has not included smoke production, oxygen depletion, or toxic products resulting from the fire and pyrolyzing materials. These effects are readily added to the technique. The development at this point also does not include fire growth, and this can be added with some complications. The development focuses on the interior panels only so that their performance features can be more clearly isolated. What the development particularly shows is that there is a relationship between fire size, material properties, and ventilation rate as indicated in the two characteristic times, τ' and τ_B . When the fire is relatively small as indicated by the relationship of the characteristic times, ventilation plays an enormous role in keeping thermal hazards at a minimum. This is shown most clearly in equation 18. However, a relatively large fire compared to the ventilation constant would lead to a situation where the cooling capability is ineffectual.

As to pyrolysis of wall lining materials, there is potentially an ablative cooling role. Whether pyrolysis effects should be considered in design would involve a more thorough evaluation of potential effects related to toxicity and flammability of the pyrolysis products of a given panel material system.

Besides analysis of oxygen depletion effects and gas injection from the walls, a more detailed development of this technique would have to include an appropriate heat loss term for heat transferred from enclosure gases to the seats. Because of their bulk and surface area, the seats might be expected to perform a function at least equivalent to the wall and ceiling panels. This would be true even if they were covered with advanced fire blocking materials. Inclusion of seats would also include the trays and seat frames. To get the overall heat transfer effects of all materials in the cabin, the more detailed approach in reference 3 might be used.

CONCLUSIONS

The application of perfect stirrer analysis to fires in ventilated aircraft cabins leads to four conclusions.

1. The ventilation rate is a major variable in fire hazard development.
2. The wall and ceiling panels play a major role in cooling the enclosure.
3. The outflow ports in test articles are locations of primary importance for locating sensors to describe the history of the fire growth.
4. Small-scale fire tests that yield thermal conductivity as part of their output are needed for evaluating panel performance in fires.

REFERENCES

1. Cooper, L. Y., The Development of Hazardous Conditions in Enclosures with Growing Fires, NBSIR 82-2622, December 1982.
2. Cooper, L. Y., A Mathematical Model for Estimating Available Safe Egress Time in Fires, Fire and Materials, v.6, nos. 3 & 4, September/December 1982.
3. Quintiere, J. G., A Simple Correlation for Predicting Temperature in a Room Fire, NBSIR 83-2712, June 1983.
4. Harkleroad, M., Quintiere, J., and Walton, W., Radiative Ignition and Opposed Flow Flame Spread Measurements on Materials, DOT/FAA/CT-83/28, August 1983.
5. Ramohalli, K., and Mink, M., Thermal Performance Modification of Composite Materials, AIAA Paper 79-0018 presented at the 17th Aerospace Sciences Meeting, New Orleans, January 1979.
6. Tustin, E. A., Development of Fire Test Methods for Airplane Interior Materials, NASA CR-14568, October 1978.

7. Spieth, H. H., Gaume, J. G., Luoto, R. E., and Klinck, D. M., A Combined Hazard Index Fire Test Methodology for Aircraft Cabin Materials, Volumes I and II, DOT/FAA/CT-82-36, April 1982.

8. Huggett, C., Time-Dependent Fire Behavior of Aircraft Cabin Materials, FAA/RD/77-99, December 1977.

9. Blake, D. R., and Hill, R. G., Fire Containment Characteristics of Aircraft Class D Cargo Compartments, DOT/FAA/82-156, March 1983.